Alignment of molecules in gaseous transport: Alkali dimers in supersonic nozzle beams

M. P. Sinha*, C. D. Caldwell†, and R. N. Zare

Department of Chemistry, Columbia University, New York, New York 10027
(Received 20 February 1974)

From measurements of the degree of polarization of the molecular fluorescence, it is shown that one can determine the coefficients of the first three even-ordered Legendre polynomials in the expansion of the spatial distribution of J vectors (M_J population), $n(\theta)=1 + a_2P_2(\cos\theta) + a_4P_4(\cos\theta)$, where θ is the angle between the angular momentum vector J of the molecule and the beam direction. This method is applied to determine the alignment of Na_2 molecules in a supersonic nozzle beam generated by expansion of sodium vapor through a converging nozzle (throat diameter = 0.375 mm and channel length = 0.750 mm) with stagnation temperature (oven temperature) up to $\sim$1015°K, corresponding to stagnation pressures (oven pressures) up to $\sim$155 torr. The 4880 Å line of a cw argon-ion laser is used to excite the transition ($v''=3$, $J''=43 \rightarrow v'=6$, $J'=43$) in the $B\,^1\Pi_u$–$X\,^1\Sigma_g^+$ band system of Na_2 molecules and the degree of polarization of a single line of the resulting fluorescence series (Q series) is measured as a function of (1) stagnation pressure p_0 and (2) the angle θ_0 between the electric vector of the exciting laser light and the molecular beam direction. A decrease in the degree of polarization from its isotropic value of 0.50 for $\theta_0=0$ to a value of 0.44 at a stagnation pressure of 155 torr is found, showing increasing alignment of dimer molecules with their angular momenta preferentially pointing perpendicular to the beam direction. At the stagnation pressure of 155 torr the coefficients of the Legendre polynomials are found to be $a_2=-0.203\pm0.006$ and $a_4=-0.14\pm0.03$. For this distribution the ratio of molecules with angular momentum J parallel and perpendicular to the beam axis is $\sim$2:3. Classical models involving the nonreactive collisions between hard spheres (atoms) and ellipsoids of revolution (molecules) and the chemical exchange between atoms and dimers predict the production of alignment in qualitative agreement with experiment.

I. INTRODUCTION

A. Review of molecular alignment in gaseous flow

If the particles in a spatially homogeneous medium are randomly oriented, then the medium is optically isotropic. By this we mean that the velocity of propagation (index of refraction), the absorption coefficient (optical rotatory power), and the fluorescence intensity (degree of polarization) are independent of the orientation of the polarization vector of a light beam incident on the medium. However, if the particles in the medium possess rotational degrees of freedom (internal angular momenta) and if the interaction between particles (intermolecular potential) depends on both separation and orientation of the particles, then as the medium flows in response to some gradient in temperature, pressure, concentration, etc., the interactions between particles cause a partial alignment (polarization) of the internal angular momentum J of the ensemble of particles with respect to the flow direction. This phenomenon is well known in liquids, having been first observed in 1877 by Maxwell[1] who measured the birefringence of a streaming colloidal suspension of Canada Balsam. However, the observation of similar phenomena in gas transport processes is much more difficult because of the smallness of the effect and consequently its investigation was delayed by many years.

In 1930, Senftleben[2] found that the thermal conductivity of O_2 changed by a few parts per thousand upon the application of a magnetic field at right angles to the flow direction. Subsequent experiments on paramagnetic molecules by Senftleben and others showed that an external electric or magnetic field could alter transport coefficients by partially destroying the alignment of the internal angular momenta of the molecules set up by the flow (gradient) through the precession of the angular momentum about the external field direction. In 1962, Beenakker, Scoles, Knaap, and Jonkman[3] demonstrated that these indirect observations of the polarization of the internal angular momenta by transport processes were not restricted to paramagnetic species but occurred as well for diamagnetic molecules. This discovery sparked a resurgence of interest in this topic, leading to many notable experiments, particularly by the molecular physics group at Leiden, on the effect of external fields on transport coefficients, a subject which is now commonly referred to collectively as the Senftleben–Beenakker effect.[4]

This revival of experimental interest was accompanied also by significant theoretical advances. A description of the transport processes for diatomic and polyatomic gases requires that the Boltzmann equation for monoatomic gases be replaced by a new kinetic equation which includes explicitly the degenerate internal angular momentum states of the molecules. The basic equation required for this purpose was derived in 1957 by Waldmann[5] and in 1960 by Snider.[6] From the Waldmann–Snider equation it follows that the internal angular momenta of nonspherical particles become aligned during flow. This fact was first noticed by Waldmann[7] in connection with the diffusion of particles with spin and by Kagan and Afanasev[8] in connection with the heat conduction of an ensemble of classically rotating molecules.

A major obstacle to the measurement of internal angular momentum effects in gas transport processes is

the smallness of the effect caused by the lack of sensitivity of bulk transport coefficients to partial alignment of the internal angular momentum states of the molecules. A second drawback to the use of the Senftleben–Beenakker effect is the difficulty of interpreting the measurements because of the rather complicated manner in which the transport coefficients are related through the Waldmann–Snider equation to the partial alignment of the internal angular momenta. Other means of obtaining information about the internal angular momentum tensor polarization and its collisional relaxation are provided by pressure broadening studies of the depolarized component of the Rayleigh scattering, the rotational Raman effect, and the resonant infrared and microwave absorption.[9,10] In addition, gas-phase NMR studies[11] as well as nonresonant microwave absorption studies[12] may be employed.

However, the most direct information on the polarization of the internal angular momenta of nonspherical molecules under transport has been provided by birefringence studies. In 1969 Hess[13] was able to show, starting from the Waldmann–Snider equation, that for a gas of linear molecules with viscosity η and temperature T, undergoing flow, the difference in the index of refraction Δn is related to the velocity gradient ∇v by

$$\Delta n = 2\pi/(15)^{1/2}(\alpha_{\parallel} - \alpha_{\perp})(\omega_{\eta T}/\omega_T)(\eta/kT)\nabla v\,. \qquad (1)$$

Here $(\alpha_{\parallel} - \alpha_{\perp})$ is the difference between the molecular polarizabilities parallel and perpendicular to the molecular axis, the relaxation coefficient $\omega_{\eta T}$ is a measure of the speed at which angular momentum tensor polarization is produced, and ω_T is a measure of the decay rate of the angular momentum polarization. Experimental verification of streaming birefringence in a gas was first obtained in 1971 by Baas[14] who measured Δn for CO_2 contained between two coaxial cylinders, one of which is rotating with respect to the other. From this experiment Baas was able to deduce the sign and magnitude of the ratio $(\omega_{\eta T}/\omega_T)$, demonstrating that the CO_2 molecules are preferentially aligned with their internal angular momenta perpendicular to the velocity gradient. This is in accord with the physical model suggested by Gorter,[15] namely, that the rotating molecules could be viewed as disks which slip by each other more easily (i.e., have the smallest collisional cross section) when the angular momentum vectors of the disks lie in a plane at right angles to the flow direction.

Recently Steinfeld, Korving, and co-workers[16] have pointed out that supersonic flows, like those in a nozzle beam,[17] hold promise for the production of significant molecular alignment, caused by the presence of a large velocity gradient in the generation of the beam. They have applied this idea to the I_2 molecule. Here one of the lines of the argon-ion laser excites I_2 fluorescence in the beam and the total fluorescence intensity is measured as a function of an applied magnetic field which rotates the plane of alignment of the I_2 molecule with respect to the fixed polarization of the laser beam. Preliminary results indicate that a small extent of molecular alignment may be present: the change in total fluorescence with applied field is found to be on the order of a few tenths of one percent.[16]

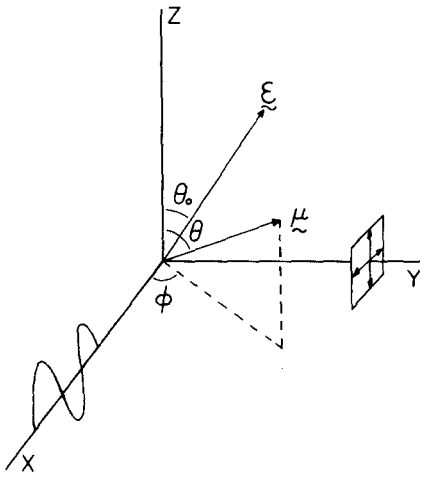

FIG. 1. Geometrical setup for the measurement of degree of polarization. The light propagates along the x axis and is plane polarized so that its electric vector, $\mathcal{E}$, makes an angle θ_0 with respect to the z axis. The molecules are represented by the Hertzian dipole oscillator μ having the spherical polar angles θ and φ. Fluorescence is observed along the y axis where the components of fluorescence intensities plane polarized parallel to the z axis and parallel to the x axis are measured.

For some time we have been interested in the characterization of the internal state distribution of alkali dimers in nozzle beams. The initial expansion through the nozzle is very closely approximated by an isentropic (adiabatic reversible) process.[18] The adiabatic nature of the expansion implies that the total enthalpy of the system remains constant. That is, $h_0 = h + \frac{1}{2}v^2$, where h_0 is the stagnation enthalpy per unit mass, h is the enthalpy per unit mass at any point in the expansion, and v is the flow velocity. Thus we see that the internal enthalpy of the system gets converted into translational energy of the beam. From fluorescence studies we have been able to measure both the vibrational and rotational distribution of alkali dimers in a nozzle beam. We find that the internal states of these dimers are appreciably cooled.[19] For example, in the case of Na_2, $T_{vib} = 153 \pm 5\,^{\circ}K$ and $T_{rot} = 55 \pm 10\,^{\circ}K$ at a stagnation temperature of 920 °K, corresponding to a stagnation pressure of 50 torr of sodium. As an extension of these earlier experiments, we have carried out measurements on the spatial alignment of the dimers. This has been accomplished by measuring the degree of polarization P of the laser-induced fluorescence. The quantity P, as shown below, is a sensitive function of the spatial distribution (M_J population) of the molecules in a rotational level J. This technique permits what we believe to be the most direct determination of the alignment of molecules in gaseous transport.

B. Dependence of polarization of fluorescence on the spatial distribution of molecules

Traditionally, polarization measurements are carried out using a right angle geometry (see Fig. 1). In this case a beam of plane polarized light propagates along the x axis with its electric vector pointing along the z axis, and the fluorescence is observed along the y axis. Then the degree of polarization P is defined[20,21] to be

$$P = (I_{\parallel} - I_{\perp})/(I_{\parallel} + I_{\perp}) , \tag{2}$$

where $I_{\parallel}$ is the intensity of the fluorescence plane polarized parallel to the electric vector of the incident light and $I_{\perp}$ is the intensity of fluorescence plane polarized perpendicular to that direction. Equation (2) applies to a highly specialized geometry of propagation, excitation, and observation. For the purpose of this work we find it convenient to consider a less restrictive definition of the degree of polarization. Although the direction of the quantization axis in any physical system is arbitrary, there is often one choice which is natural for the description of the system. For an isotropic distribution of molecules the electric vector of the incident beam provides an obvious choice for the quantization axis. However, in our experiment the direction of the nozzle beam proves to be the simplest choice of quantization axis which facilitates computations. The electric vector $\mathcal{E}$ need not necessarily lie along this axis but may make an arbitrary angle θ_0 with respect to the beam direction, chosen to be the z axis, as shown in Fig. 1. An observer along the z axis no longer measures $I_{\parallel}$ and $I_{\perp}$ unless θ_0 is equal to zero degrees, but still resolves the fluorescence into two intensity components. We call these intensity components I_z and I_x, where I_z is the intensity of fluorescence which is plane polarized along the molecular beam axis and I_x is the intensity of fluorescence which is polarized along the incident laser beam. We then define a more generalized degree of polarization

$$\mathcal{P}(\theta_0) = (I_z - I_x)/(I_z + I_x) . \tag{3}$$

For diatomic molecules with large rotational angular momenta the absorption and emission of light may be approximated by replacing the molecule with a classical Hertzian dipole oscillator. From symmetry arguments it follows that the dipole oscillator must lie along the internuclear axis for a parallel type transition (e.g., $\Sigma - \Sigma$), whereas the dipole oscillator must lie in a plane at right angles to the internuclear axis for a perpendicular type transition (e.g., $\Sigma \rightarrow \Pi$ or $\Pi \rightarrow \Sigma$). In the latter case we may distinguish two additional possibilities: for a Q transition ($\Delta J = 0$) the dipole oscillator lies along the angular momentum vector $\mathbf{J}$, which is, classically, at right angles to the internuclear axis, while for R and P transitions ($\Delta J = +1$ and -1, respectively) the dipole oscillator lies in the plane of rotation, perpendicular to both the internuclear axis and the angular momentum $\mathbf{J}$. Because we primarily study a resonance fluorescence process ($\Sigma \rightarrow \Pi \rightarrow \Sigma$) in which both the absorption and emission involve $\Delta J = 0$ transitions ($Q\uparrow$, $Q\downarrow$),[22] we specialize the following considerations to this case.

Let us denote the distribution of dipole oscillators by $n(\theta, \varphi)$, where θ, φ are the polar angles measured in the coordinate system in which the z axis lies along the molecular beam axis. Because the distribution of molecules in the beam must have azimuthal symmetry, $n(\theta, \varphi)$ is independent of φ and will henceforth be written simply as $n(\theta)$. Note that the distribution of angular momentum vectors of the molecule is identical to $n(\theta)$ because the dipole oscillators lie along J for a ($Q\uparrow$, $Q\downarrow$) fluorescence process.

Let $\hat{\mu}$, $\hat{\mathcal{E}}$, $\hat{z}$, and $\hat{x}$ denote unit vectors along the dipole oscillator, the electric field of the incident light beam, the z axis, and the x axis, respectively. The intensities I_z and I_x may then be expressed in terms of the dipole oscillator distribution $n(\theta)$ by the following integrals:

$$I_z = K \int n(\theta)(\hat{\mathcal{E}} \cdot \hat{\mu})^2 (\hat{\mu} \cdot \hat{z})^2 d\Omega \tag{4}$$

and

$$I_x = K \int n(\theta)(\hat{\mathcal{E}} \cdot \hat{\mu})^2 (\hat{\mu} \cdot \hat{x})^2 d\Omega , \tag{5}$$

where K is a constant independent of angle. With the help of Fig. 1 and the spherical harmonic addition theorem we see that:

$$\hat{\mu} \cdot \hat{\mathcal{E}} = \cos\theta \cos\theta_0 + \sin\theta \sin\theta_0 \cos[(\pi/2) - \varphi], \tag{6}$$

$$\hat{\mu} \cdot \hat{z} = \cos\theta , \tag{7}$$

$$\hat{\mu} \cdot \hat{x} = \sin\theta \cos\varphi . \tag{8}$$

The distribution $n(\theta)$ may be expanded in a complete set of Legendre polynomials, $P_l(\cos\theta)$.

$$n(\theta) = \sum_{l=0}^{\infty} b_{2l} P_{2l}(\cos\theta) . \tag{9}$$

In this expansion only Legendre polynomials of even order occur because the dipole radiation is symmetric about a plane normal to the flow axis. Substituting Eqs. (6)–(9) into Eqs. (4) and (5) we obtain the expressions:

$$I_z = \pi K \left[\cos^2\theta_0 \left(\frac{4}{5} b_0 + \frac{16}{35} b_2 + \frac{32}{315} b_4 \right) + \sin^2\theta_0 \left(\frac{4}{15} b_0 + \frac{4}{105} b_2 - \frac{16}{315} b_4 \right) \right] \tag{10}$$

$$I_x = \pi K \left[\cos^2\theta_0 \left(\frac{4}{15} b_0 + \frac{4}{105} b_2 - \frac{16}{315} b_4 \right) + \sin^2\theta_0 \left(\frac{4}{15} b_0 - \frac{8}{105} b_2 + \frac{4}{315} b_4 \right) \right] . \tag{11}$$

Note that only the first three terms of the expansion in Eq. (6) contribute to the observed intensities I_z and I_x. This is a general result: electric dipole resonance fluorescence only allows one to determine the contributions from these three polynomials due to the nature of the absorption and emission process and the orthogonality properties of the Legendre polynomials. Substituting Eqs. (10) and (11) into Eq. (3) we obtain the result:

$$\mathcal{P}(\theta_0) = \frac{\cos^2\theta_0(42 + 33a_2 + 12a_4) + \sin^2\theta_0(9a_2 - 5a_4)}{\cos^2\theta_0(84 + 39a_2 + 4a_4) + \sin^2\theta_0(42 - 3a_2 - 3a_4)} , \tag{12}$$

where $a_2 = b_2/b_0$ and $a_4 = b_4/b_0$. Thus it is possible by measuring $\mathcal{P}(\theta_0)$ at two values of θ_0 to determine the coefficients a_2 and a_4, i.e., the relative contributions of the Legendre polynomials $b_0 : b_2 : b_4$.

Based on this formalism we have characterized the alignment of molecules in an alkali nozzle beam by performing degree of polarization measurements of the laser-induced fluorescence. In Sec. II we describe the experimental conditions and in Sec. III we present the results of the molecular alignment as a function of stagnation pressure p_0 (vapor pressure in the oven) and as a function of the angle θ_0 at the highest stagnation

pressures. In Sec. IV we develop a classical model for alignment involving the inelastic collisions between hard spheres (atoms) and hard ellipsoids of revolution (dimers). We also consider a classical model for the production of alignment through chemical exchange collisons. Finally in Sec. V we discuss briefly the implications such flow alignment may have for various processes involving gaseous transport.

II. EXPERIMENTAL

A. Beam apparatus and optics

The molecular beam apparatus for generating a supersonic nozzle beam of alkali molecules has been described in some detail previously.[19] Consequently, we only summarize here the main points. The alkali metal is heated in a stainless steel double oven. We use sodium metal from Matheson, Coleman & Bell with a stated purity of 99.9%. The vapor from the oven forms a supersonic beam after passing through a converging nozzle (throat diameter 0.375 mm, channel length 0.750 mm) followed by a series of concentric holes (collimators) cut in water-cooled and liquid-nitrogen-cooled shields. Further definition of the beam is provided by additional copper collimators mounted on the liquid-nitrogen-cooled shield. With this setup, the divergence angle of the beam is about 4°. The oven is supported by four tungsten pins and is carefully positioned in line with the collimators. The final adjustment of the nozzle is made with a He–Ne line-up laser. The heights of the pins are adjusted such that the horizontal beam of the laser is reflected back on itself from the nozzle. This ensures that the central flow line of the molecular beam is horizontal to better than 0.5 deg. The beam emerges into an expansion chamber consisting of a large Pyrex bell jar (16.8 cm diam). The metal vapor is mostly cryopumped by the liquid-nitrogen-cooled shields. A background pressure of about 1×10^{-6} torr is maintained in the expansion chamber with a 6 in. oil diffusion pump (2400 l/sec) while the beam is on.

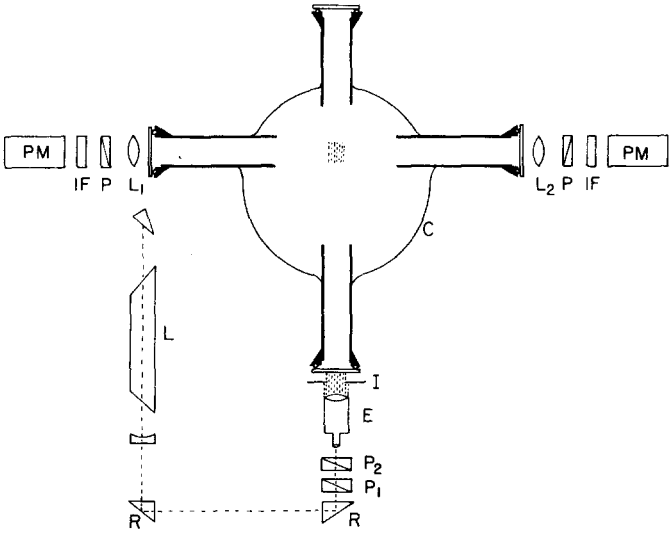

FIG. 2. Schematic diagram of the experimental arrangement: L = Laser; L_1, L_2 = Lenses; P_1, P_2, P = polarizers; PM = photomultipliers; C = expansion chamber; E = beam expander; I = Iris; IF = interference filters; R = prisms.

Fluorescence of the sodium dimers is excited in the expansion chamber by intersecting the nozzle beam with a light beam from a multimode cw argon ion laser (Control Laser Corporation model 906) directed perpendicular to the nozzle beam. The natural width of the Na_2 absorption line is larger than the hyperfine splittings so that the laser does not frequency-select hyperfine levels. The laser beam has a long-term drift of less than 1%. The region of intersection of the two beams lies far downstream from the nozzle (~12 cm) so that the internal state distribution characterizing the nozzle expansion has been frozen. The Na_2 $B^1\Pi_u - X^1\Sigma_g^+$ fluorescence[23] is detected at right angles to both the light beam and the molecular beam. To facilitate this optical setup, four Pyrex sidearms (4 cm i.d., 17 cm long) are attached to the expansion chamber to form a cross whose plane is perpendicular to the nozzle beam direction. The sidearms are carefully positioned to be at 90° to one another. Optically flat, strain-free Pyrex windows mounted by O rings to glass flanges cap off each sidearm. In order to minimize scattered laser light as well as unwanted fluorescence reflections the inside of each sidearm is lined with thin blackened teflon sheets. This arrangement also helps to define the direction of observation of the fluorescence.

Figure 2 is a schematic diagram of the experimental setup. The laser beam is brought to the molecular beam apparatus by means of a number of prisms that bend the light beam by 90° at each prism while preserving the light beam's polarization. The laser beam then passes through a pair of calcite polarizers (P_1, P_2) and a beam expander (E). The linear polarizers P_1 and P_2 are mounted together in a single housing so that P_2 can be rotated with respect to P_1. The former is provided with a circular dial which is marked off every degree.

In order to avoid optical pumping[24] of the molecules in the beam, the power density of the laser beam is reduced by passing it through a 10× beam expander E which is simply an ordinary 10× inverted telescope. The expanded laser beam is linearly polarized and the angle its electric vector makes with respect to the direction of the molecular beam is set by adjusting P_2. The power of the incident laser light is measured by inserting a laser-power-meter between P_2 and E in Fig. 2. No absolute power measurements are needed in the present study. Rather, the laser-power-meter helps to set the laser power so that optical pumping is avoided. This is ensured by measuring the degree of polarization of the fluorescence with decreasing laser power until it becomes independent of any further power attenuation.

B. Polarization measurement as a function of stagnation pressure p_0

We wish to measure the conventional degree of polarization P, given in Eq. (2), for various oven source pressures p_0. Because the fluorescent intensity changes with the operating conditions of the beam source, it is desirable to measure $I_\parallel$ and $I_\perp$ simultaneously rather than sequentially, as is more common. This is accomplished

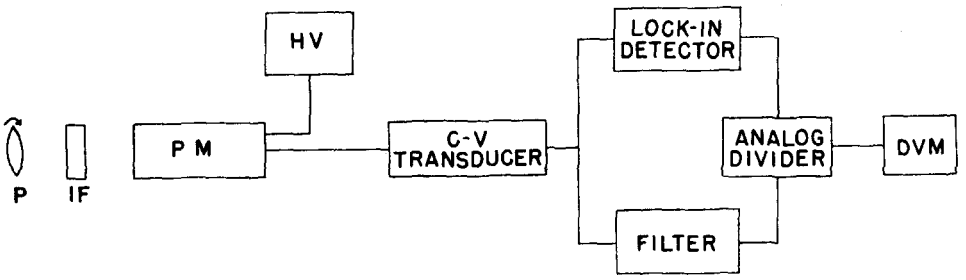

FIG. 3. Block diagram of detection electronics and the rotating polarizer. Here P = polarizer, IF = interference filter, PM = photomultiplier, HV = High voltage, C – V = Current-voltage, DVM = digital voltmeter.

by using an optical bridge as shown in Fig. 2. Here the fluorescence is viewed by two photomultipliers placed opposite to one another on either side of the sidearms of the expansion chamber. Each photomultiplier is provided with its own polarizer (Polaroid Corporation) and with its own narrow band interference filter (Corion Instrument Corp.). The latter form an identically matched pair.

The transmission of the interference filter is centered at 5287 Å. This isolates the Na_2 $B-X$ ($v'=6$, $J'=43 \rightarrow v''=14$, $J''=43$) Q line for excitation by the 4880-Å laser line and the ($v'=6$, $J'=27 \rightarrow v''=14$, $J''=28$, 26) P and R lines for excitation by the 4765-Å laser line.[25] The currents from the photomultipliers are measured by separate Keithly 417 picoammeters with a 3 sec time constant. The outputs of the picoammeters then drive a double pen chart recorder (Hewlett–Packard model 7100B). The intensities $I_{\parallel}$ and $I_{\perp}$ are traced on this strip chart recorder for varying nozzle beam operating conditions and the variation of the ratio $I_{\parallel}/I_{\perp}$ is determined.

It is to be noted that the above procedure only determines the variation of the ratio $I_{\parallel}/I_{\perp}$ with stagnation pressure. In order to determine the degree of polarization it is necessary to calibrate the optical bridge at one pressure. A rotating polarizer[26] was used to make an absolute measurement of P at the highest stagnation pressure (155 torr).

The rotating polarizer is mounted on an air-bearing (Weldon Tool Co., Cleveland, Ohio) and is rotated by a synchronous motor (2 oz./in. torque) at a frequency of 18.4 cps. The air-bearing has the advantage of virtually eliminating mechanical vibrations. Figure 3 illustrates the detection electronics. The reference signal for the lock-in amplifier (PAR HR8) is at twice the above frequency and is obtained by chopping the dc light signal falling on a photodiode. The rotating polarizer modulates the fluorescence signal also at the chopping frequency. The output of the photomultiplier consists of an ac signal superimposed on a dc signal. The ac signal is analyzed by the lock-in detector whose output is proportional to the quantity $(I_{\parallel}-I_{\perp})$. The dc signal is proportional to the quantity $(I_{\parallel}+I_{\perp})$. By taking the ratio of the two output signals with an analog divider (Burr–Brown model 4290) the degree of polarization P is obtained. The entire detection system is calibrated at $P=1$ and $P=0$ by using a spinning light bulb with and without a sheet of Polaroid. The calibration at $P=1$ is made by placing the Polaroid with its optical axis parallel to the beam direction. The phase angle of the reference signal is adjusted to give zero phase difference between the reference and modulated fluorescence signals. This corresponds to a maximum output of the lock-in for $P=1$ and zero output for $P=0$.

C. Polarization measurement as a function of the angle between the electric vector and the molecular beam

The measurement of $\mathcal{P}$ for different values of the angle θ_0 (see Sec. IB) was made at the highest stagnation pressure p_0. Since $\mathcal{P}$ is a sensitive function of θ_0 for $\theta_0 > 15°$, it is important to know the exact value of the latter. This is accomplished in the following manner. The transmission axis, defined to be parallel to the polarization vector of the transmitted light, is determined for the final polarizer P_2 by passing a linearly polarized argon-ion laser beam through it. The polarizer P_2 is then mounted on an optical bench such that its transmission axis lies in the horizontal plane and the polarization vector of the transmitted light is as closely parallel to the molecular beam (z axis) as possible. The small offset angle α between the beam direction (z axis) and the electric vector $\mathcal{E}$ of the incident laser light in the horizontal plane is determined by first measuring I_z at an angle θ_1 (in the first quadrant) of P_2 and then finding the angle setting $(2\pi - \theta_2)$ (in the fourth quadrant) which exactly reproduces the intensity I_z. The angle α

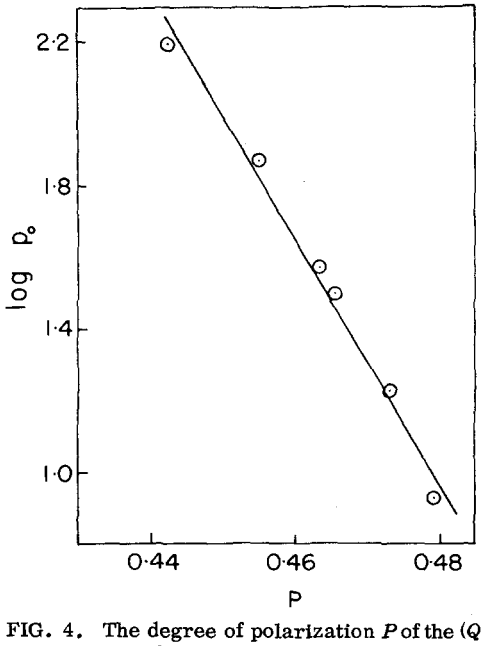

FIG. 4. The degree of polarization P of the ($Q\uparrow$, $Q\downarrow$) fluorescence as a function of the logarithm of the stagnation pressure, log p_0. Open circles are the experimental points and the solid line is the least squares fit to them.

TABLE I. Measured values of the general degree of polarization $\mathcal{P}(\theta_0)$ for different angles θ_0. The errors represent one standard deviation in ten measurements of each $\mathcal{P}(\theta_0)$.

θ_0 (degrees)	$\mathcal{P}(\theta_0)$	$\mathcal{P}_{iso}(\theta_0)$
0°	0.443 ± 0.011	0.500
15°	0.421 ± 0.025	0.485
30°	0.374 ± 0.004	0.433
45°	0.269 ± 0.003	0.333
60°	0.149 ± 0.004	0.210

is given by $\frac{1}{2}(\theta_2 - \theta_1)$. With this procedure we could establish the angle θ_0 with an uncertainty of less than 0.5 deg.

The fluorescence detection optics is essentially the same as for one arm of the optical bridge described above (see II B) but with the difference that the analyzing polarizer consists of a pair of matched Polaroid sheets. These are mounted on a single frame and can be translated back and forth in front of the phototube, as slides in a slide projector.[24] These expose exactly the same areas of the polarizers in the two cases, one giving I_z and the other I_x. Several pairs of measurements, I_z and I_x, are made for each setting of θ_0 and $\mathcal{P}$ is calculated from them according to Eq. (3). Although these measurements of $\mathcal{P}$ as a function of θ_0 are sequential, the results at the highest stagnation pressure are in agreement with those obtained from the optical bridge at $\theta_0 = 0$. Under these conditions (highest p_0) the fluorescence intensity is at a maximum and does not change with time because of the stable beam characteristics.

III. RESULTS

Using the optical bridge arrangement in conjunction with the rotating polarizer as described in Sec. II B, we have measured the degree of polarization P of the Q fluorescence series originating from the $(v' = 6,\ J' = 43)$ vibrational–rotational level of the $B\,^1\Pi_u$ state of Na_2. Figure 4 shows the variation of P with the stagnation pressure p_0. The degree of polarization is observed to decrease from a value of 0.48 at a stagnation pressure $p_0 = 8$ torr to $P = 0.44$ at $p_0 = 155$ torr. Moreover, P appears to vary linearly with $\log p_0$. We do not understand why the degree of polarization has this functional dependence on p_0. Unfortunately, we were not able to pursue this point because of the limitation on the oven temperature we could reach with the present setup. Determination of P for $p_0 < 8$ torr could not be made because of the weakness of the fluorescence signal at such low pressures. However, extrapolation of $\log p_0$ to zero ($p_0 \sim 1$ torr) yields $P = 0.507 \pm 0.003$, where the uncertainty represents one standard deviation. This value is very close to the isotropic value[22] and is what we would expect at the low pressure limit because, under these conditions, the beam is nearly effusive and consequently molecules in it should be isotropically distributed.

As can be seen from Fig. 4, the sodium dimers become increasingly aligned with increasing stagnation pressure. If the distribution $n(\theta)$ of angular momentum vectors J has a maximum in a plane perpendicular to the beam direction and a minimum forward and backward along the beam direction, and if the distribution varies monotonically between these two extremes, then it can be shown that the degree of polarization must be less than its isotropic value of 0.50. Hence the observation of the variation of P with p_0 is consistent with the picture that the molecules are increasingly aligned with their J vectors oriented perpendicular to the flow direction. In order to determine this distribution in more detail we have carried out general degree of polarization measurements, $\mathcal{P}(\theta_0)$, (see Sec. I B) at the highest stagnation pressure, for which the signal to noise ratio is most favorable.

Table I lists the value of $\mathcal{P}$ for different values of the angle θ_0 between the beam direction and the electric vector of the exciting laser light. These measurements were performed at a stagnation temperature of 1013 °K, corresponding to a stagnation pressure p_0 of approximately 155 torr.[27] The uncertainties in Table I represent one standard deviation. In the last column in Table I we include the value of the generalized degree of polarization which would be found for an isotropic distribution of molecules, $\mathcal{P}_{iso}(\theta_0)$.

From each entry in Table I we obtain, using Eq. (12), one equation relating the expansion coefficients a_2 and a_4 to $\mathcal{P}(\theta_0)$. Each pair of equations resulting from two different $\mathcal{P}(\theta_0)$ measurements may be solved for a_2 and a_4. In Table II we present the results of such a treatment, where the uncertainties in the values of a_2 and a_4 are calculated from the uncertainties in $\mathcal{P}(\theta_0)$ using the theory of propagation of errors.[28] It is important to note that some pairs of θ_0 are more sensitive for determining a_2 and a_4 than others. To obtain average values of a_2 and a_4 we weight each determination by the inverse of its variance. (See Table II.) In this manner we obtain the final values:

$$a_2 = -0.203 \pm 0.006 \tag{13}$$

and

$$a_4 = -0.14 \pm 0.03\ . \tag{14}$$

TABLE II. The coefficients a_2 and a_4 calculated from Eq. (12) using two different values of $\mathcal{P}(\theta_0)$. Here w_2 and w_4 are their respective weights and the errors in a_2 and a_4 are propagated from the errors in the measurement of $\mathcal{P}(\theta_0)$ (see Table I).

(θ_0', θ_0'')	a_2	$w_2 = 1/\sigma_2^2$	a_4	$w_4 = 1/\sigma_4^2$
0, 15	−0.3511 ± 1.2689	2.37×10^{-5}	0.0688 ± 1.9797	2.65×10^{-4}
0, 30	−0.1370 ± 0.1164	2.82×10^{-3}	−0.2606 ± 0.2609	1.53×10^{-2}
0, 45	−0.2252 ± 0.0317	3.79×10^{-2}	−0.1249 ± 0.1305	6.11×10^{-2}
0, 60	−0.1985 ± 0.0133	2.16×10^{-1}	−0.1659 ± 0.0835	1.48×10^{-1}
15, 30	−0.0749 ± 0.3439	3.23×10^{-4}	−0.4074 ± 0.8109	1.58×10^{-3}
15, 45	−0.2176 ± 0.0732	7.13×10^{-3}	−0.1614 ± 0.3414	8.93×10^{-3}
15, 60	−0.1996 ± 0.0154	1.62×10^{-1}	−0.1925 ± 0.2042	2.49×10^{-2}
30, 45	−0.2552 ± 0.0290	4.52×10^{-2}	0.0192 ± 0.1005	1.03×10^{-1}
30, 60	−0.1966 ± 0.0125	2.43×10^{-1}	−0.1194 ± 0.0488	4.37×10^{-1}
45, 60	−0.2015 ± 0.0116	2.85×10^{-1}	−0.2388 ± 0.0722	2.00×10^{-1}

We see that the coefficient a_2 is well known since its magnitude is approximately thirty times its standard deviation; the coefficient a_4 is less certain, but we are confident, since its magnitude is approximately five times its standard deviation that we have obtained a reliable (nonzero) estimate for it. Although a_4 is less than a_2, its effect is clearly nonnegligible and this fact, together with the observation that a_2 and a_4 are of the same sign, suggests that the expansion of $n(\theta)$ in even-ordered Legendre polynomials may not be rapidly convergent.

As mentioned in Sec. I B, we can only determine the contribution of the first three Legendre polynomials to the distribution of J vectors of the molecules. We denote this contribution by

$$n_{\text{partial}}(\theta) = 1 + a_2 P_2(\cos\theta) + a_4 P_4(\cos\theta). \quad (15)$$

Using the values of a_2 and a_4 given in Eqs. (13) and (14), we have plotted $n_{\text{partial}}(\theta)$ in Fig. 5. If we assume that $n_{\text{partial}}(\theta)$ is a good representation of $n(\theta)$, it is apparent that the angular momentum vectors J preferentially point away from the beam axis rather than along it. Indeed, the ratio of the number of molecules with angular momentum J parallel and perpendicular to the beam axis is ~2:3. The distribution $n_{\text{partial}}(\theta)$ shows maxima at $\theta = \pi/3$ and $\theta = 2\pi/3$, but these maxima are not strongly pronounced. Instead the distribution is rather flat between $\pi/3$ and $2\pi/3$. Of course, the actual distribution $n(\theta)$ may be more peaked than $n_{\text{partial}}(\theta)$ about $\theta = \pi/2$.

Much effort was spent to ascertain that the values derived for a_2 and a_4 are reliable and reproducible. There are three important sources of systematic errors: (1) optical pumping; (2) spurious polarizations; and (3) geometrical misalignment. We are confident that the errors introduced by optical pumping are negligible. Care was taken to attenuate the power of the laser beam until the degree of polarization measurements were independent of this variable. Indeed, if optical pumping were present, we would expect[24] the degree of polarization for Q-line fluorescence to increase with increasing p_0, opposite to the effect which we have seen. We have measured the degree of polarization of both the Q-line and the P- and R-line fluorescence using different argon-ion laser lines (see Sec. II B). We find the degree of polarization of the P and R lines to increase with increasing p_0, while the degree of polarization of the Q-line fluorescence decreases. These results are what would be expected for the increasing alignment of the molecules in the beam but cannot be explained by optical pumping. The effect of spurious polarizations has been minimized by using strain-free optical components and by reducing the amount of reflected fluorescence and laser light entering the detector through the use of light baffles. We believe that spurious polarizations have negligible effect on the results because the absolute degree of polarization extrapolated to the low-pressure limit for the beam has the isotropic value in accord with theory. Moreover, we would expect any spurious polarization to be a constant of the system and not vary with p_0.

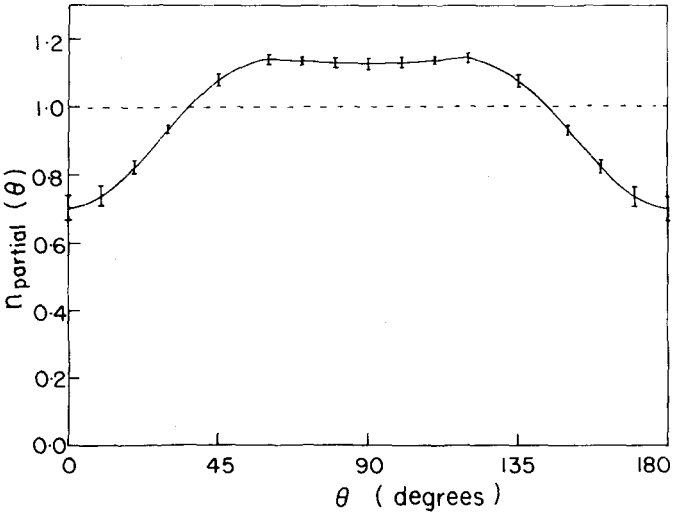

FIG. 5. Plot of experimentally determined $n_{\text{partial}}(\theta)$ vs θ with $a_2 = -0.203$ and $a_4 = -0.14$. The error bars represent one standard deviation. The dashed line corresponds to an isotropic distribution. The area underneath the $n_{\text{partial}}(\theta)$ distribution has been normalized to have the same area as for the isotropic distribution.

The most important source of systematic error arises from the possible geometrical misalignment of the laser beam and the molecular beam. Extreme care has to be exercised to make the electric vector of the plane-polarized laser beam have a known angle θ_0 with respect to the nozzle beam direction. In our earliest runs the degree of polarization was found to vary because insufficient attention was given to this point. However, using the alignment procedures described in Sec. II B, we have overcome this problem, and our measurements are reproducible within the statistical uncertainty (one standard deviation). It is also necessary for the polarization analyzers to be parallel and perpendicular to the beam flow, but this is readily achieved. Consequently, we believe that we have removed these sources of systematic error from our measurements.

IV. CLASSICAL COLLISION MODELS FOR PRODUCTION OF ALIGNMENT

There are a number of processes simultaneously occurring in the formation of an alkali dimer nozzle beam. There is a pressure gradient set up and the atoms and molecules undergo a successively decreasing number of collisions as they travel along the beam. In addition to collisions which have the effect of converting internal energy into directed translational energy, there is a chemical formation of dimer molecules[29] together with a concentration of the heavier dimers along the central streamline due to the difference in diffusion rates.[30] Moreover, for the high Reynolds numbers[31] characterizing our nozzle beams we have a nonviscous flow. Initially the monomers and dimers must have different velocities so that they "slip by" each other in the course of the expansion.

In the same spirit as Gorter's earliest suggestion[15] on the origin of the Senftleben effect we can imagine a continuum mechanics explanation for this alignment much like streamers on a fan are aligned in the wind such that they offer the least resistance to the airflow. Con-

tinuum mechanics must have its basis in microscopic processes and with this in mind we have undertaken to develop a simplistic model for the alignment of linear molecules by the expansion of a mixture of such molecules with atoms in a nozzle beam. We first consider in some detail how nonreactive scattering processes might contribute to the flow alignment. Then we briefly discuss the possible role of "reactive" scattering in which atoms are exchanged in the collision between an alkali atom and an alkali dimer.

A. Nonreactive collisions

The mechanism for nonreactive alignment depends on the angular part of the intermolecular potential. Unfortunately, for an alkali atom and an alkali dimer the radial part of the intermolecular potential can only be estimated and the angular part is unknown. We do know, however, that the charge distribution of a molecule in a $^1\Sigma$ state has cylindrical symmetry about the internuclear axis. Viewed from outside the distribution, the molecule has the geometric shape of an ellipsoid of revolution with the internuclear axis forming the major axis of the ellipsoid. Suppose a mixture of atoms and molecules flow together, each with its own velocity, in a beam. Then the probability per unit length that a molecule makes a collision with an atom will depend on the orientation of the molecule with respect to the relative velocity vector. We idealize this situation by considering the classical collisions between hard spheres (atoms) and hard ellipsoids of revolution (linear molecules) in a one-dimensional flow.[32] If an ellipsoid is aligned such that its major (internuclear) axis is along the direction of the flow, one would expect it to undergo fewer collisions than it would if it were lined up with its internuclear axis perpendicular to the flow. The reason for this is that the cross-sectional area for collisions is greater in the latter case than in the former. The difference in the collision probability for each orientation should be a function of the ratio of the semiminor to semimajor axes of the ellipsoid (molecule) since this will determine the difference in the area exposed to the spheres with which it collides. These considerations lead us to expect that the ellipsoids tend to lie with their major axis along the direction of the flow since this orientation offers "least resistance." This would result in J (which is perpendicular to the internuclear axis) being aligned perpendicular to the flow.

Let the semimajor and semiminor axes of the ellipsoid be denoted by a' and b' and let the relative velocity between the ellipsoid and the spheres be given by $\mathbf{v}_r$. The classical cross section for collisions is the impact area exposed perpendicular to $\mathbf{v}_r$, which has the form of an ellipse lying in the plane perpendicular to this vector. Let the sphere have a radius r. Then by defining $a = a' + r$ and $b = b' + r$ it can be seen from Fig. 6 that the impact area A is given by

$$A = \pi b (a^2 \sin^2\Theta + b^2 \cos^2\Theta)^{1/2} . \tag{16}$$

Consider a beam consisting of ellipsoids of an intensity of N particles $\sec^{-1} \cdot \mathrm{sr}^{-1}$ and spheres of density n with a relative velocity distribution $f(\mathbf{v}_r)$. The total number of collisions which the ellipsoids make in passing through a distance Δz along the beam direction z is

$$\int d\mathbf{v}_r f(\mathbf{v}_r) \sigma(\hat{v}_r) n N \Delta z , \tag{17}$$

where $\sigma(\hat{v}_r)$ is the area given above. Note that in this model σ depends only on the direction of $\mathbf{v}_r$ and not on its magnitude.

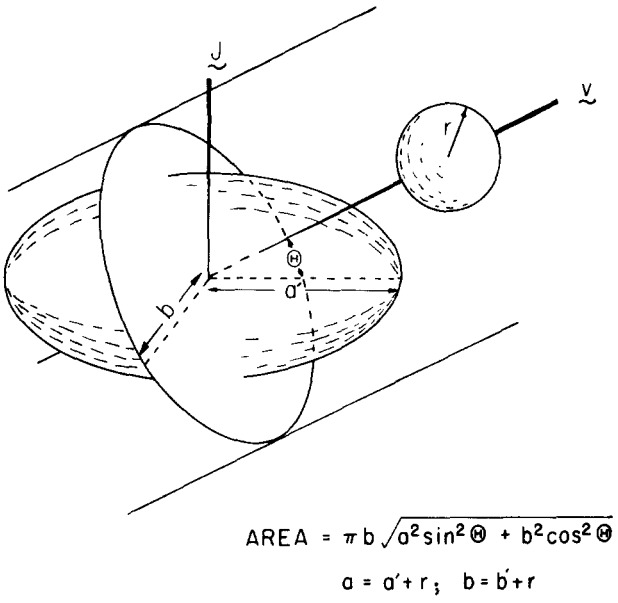

FIG. 6. Collision between an ellipsoid (semimajor axis = a' semiminor axis = b') and a sphere (radius = r) with a relative velocity v making an angle Θ with the major axis of the ellipsoid The cross section through the center of the ellipsoid shows the impact area.

We distinguish two types of collisions, "soft" and "hard." In the soft collisions the angular momentum of the ellipsoid may be only slightly altered in magnitude and direction. The small torque exerted in a soft collision will cause J to nutate about its position in such a way that its average value will be little changed. On the other hand, a hard collision may transfer a large amount of angular momentum to the molecule and the direction of the new angular momentum of the molecule has almost no memory of its original direction. Thus it is primarily the hard collisions which will be effective in causing alignment and consequently we focus our attention on this type of collision.[33] We make the crude assumption that any collision at any point on the ellipse completely randomizes J. This assumption neglects the fact that collisions at different points can change the orientation of J by different amounts. We assume further that no ellipsoid is removed from the beam by collisions, i.e., the total number of molecules is conserved.

Let $N(\theta, \varphi, z)$ be the intensity of ellipsoids with their J oriented at spherical angles θ, φ at a point z measured along the beam direction. Because of the azimuthal symmetry of the beam, $N(\theta, \varphi, z)$ will be symmetric about the z axis and the φ dependence will be omitted. As the ellipsoids pass through a distance Δz along z, the number removed from this orientation by collisions is:

$$-\int n N(\theta, z) d\mathbf{v}_r \sigma(\hat{v}_r) f(\mathbf{v}_r) \Delta z . \tag{18}$$

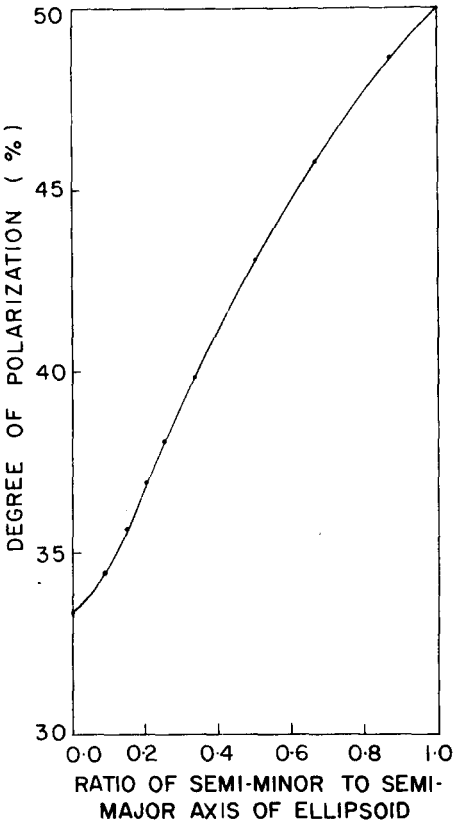

FIG. 7. Variation of the calculated degree of polarization P for $(Q\uparrow, Q\downarrow)$ fluorescence as a function of the ratio of semiminor to semimajor axis of the impact ellipse.

However, the number of ellipsoids in a particular orientation will also increase by an amount

$$+\tfrac{1}{2}\int_0^\pi \sin\theta\, d\theta \int d\mathbf{v}_r n N(\theta, z)\sigma(\hat{v}_r) f(\mathbf{v}_r)\Delta z \qquad (19)$$

due to the random distribution produced by the totality of collisions. Thus the change in the distribution at a particular orientation in an increment dz is

$$\frac{dN(\theta, z)}{dz} = -\int n N(\theta, z)\sigma(\hat{v}_r) f(\mathbf{v}_r)\, d\mathbf{v}_r + \frac{1}{2}\int_0^\pi \sin\theta\, d\theta \int n N(\theta, z)\sigma(\hat{v}_r) f(\mathbf{v}_r)\, d\mathbf{v}_r . \qquad (20)$$

Equation (20) is general for any cross section and any velocity distribution with the assumption that the effect of the collisions is only the spatial redistribution of J. For our simple case we have

$$f(\mathbf{v}_r) = \delta(v_{rx})\,\delta(v_{ry})\,\delta(v_{rz} - v), \qquad (21)$$

where v is the difference in velocities of the spheres and the ellipsoids and we assume n is constant along the flow. Using Eqs. (20) and (21) and expressing σ in terms of θ we integrate Eq. (20) over velocity to obtain the expression

$$\frac{dN(\theta, z)}{dz} = -nN(\theta, z)\pi b(a^2\cos^2\theta + b^2\sin^2\theta)^{1/2} + \frac{1}{2} n\int_0^\pi \sin\theta\, d\theta N(\theta, z)\pi b \times (a^2\cos^2\theta + b^2\sin^2\theta)^{1/2} . \qquad (22)$$

Upon examining Eq. (22) we see that with increasing distance z along the flow the number of ellipsoids lost from one orientation by collisions will approach the number the orientation gains from all the collisions. In this steady-state limit the distribution of the ellipsoids is given by

$$N(\theta) = \text{constant}/(a^2\cos^2\theta + b^2\sin^2\theta)^{1/2} \qquad (23)$$

which shows a very simple dependence on the ratio of the axes of the impact ellipse and on the angle θ which J makes with the beam axis.

For the same geometry as was used in the experimental study, we calculate the degree of polarization P [see Eq. (2)] for the $(Q\uparrow, Q\downarrow)$ transition as a function of the ratio b/a. Figure 7 illustrates these results. In the limit where $b/a = 1$, corresponding to spherical molecules, no alignment occurs, and the degree of polarization is unaltered from its isotropic value of $\frac{1}{2}$. In the limiting case where $b/a \to 0$, corresponding to "needle-like" molecules, $P \to \frac{1}{3}$. For intermediate cases the polarization is seen to decrease monotonically as the ratio b/a decreases.

Assuming that at the highest stagnation pressure we have reached the steady-state limit, then the ratio b/a may be obtained from the measured value of P. For $P = 0.44$ we find from Fig. 7 that $b/a = 0.57$. Using this ratio, we have evaluated $N(\theta)$ with the help of Eq. (23). The results are plotted (solid line) in Fig. 8. In addition we have plotted on the same figure (dashed line) the contribution from the first three non-zero terms obtained by expanding $N(\theta)$ in Legendre polynomials. This latter corresponds to the coefficients $a_2 = -0.377$, $a_4 = 0.107$. We note that this figure is qualitatively similar to Fig. 5, which is the experimentally determined contribution to $N(\theta)$ from the first three even-ordered Legendre poly-

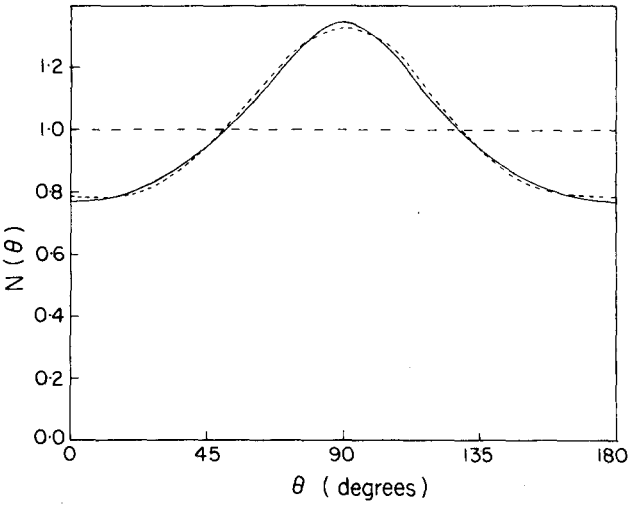

FIG. 8. Plot of the distribution $N(\theta)$ vs θ calculated from the hard collision model. The solid line represents $N(\theta)$ calculated from Eq. (23) and the dotted line is the plot of the contribution from the first three even order Legendre polynomials in the expansion of $N(\theta)$ given by the above equation. P_2 and P_4 have their coefficients as $a_2 = -0.377$ and $a_4 = 0.107$. The dashed line is an isotropic distribution. The areas underneath these curves have been normalized to have the same value.

nomials, namely, there is a pronounced depletion of the number of molecules whose J vectors point along the beam direction. However, examination of Figs. 5 and 8 reveals that the distribution $N(\theta)$ given by this model is not as broad about the perpendicular plane as is that obtained experimentally. Moreover, the above model cannot yield a negative value for a_4 for any choice of b/a, and hence this treatment must fail to reproduce in detail the observed distribution.

There are many possible reasons for the discrepancies between the distributions shown in Figs. 5 and 8. It should be borne in mind that the experimentally determined distribution, $n_{\text{partial}}(\theta)$, represents only the first three terms in the expansion of $n(\theta)$ in Legendre polynomials and the actual distribution may be more peaked. In addition, the steady-state limit may not have been reached in our experiment, and this may contribute to the breadth of the apparent distribution. A hard collision model tends to exaggerate the extent of alignment, and the distribution from a more realistic potential may be expected to be broader. It should be recalled that our treatment has been limited to collisions along the flow direction and the effect of averaging over possible collision directions would again be expected to lead to a broader distribution.[34] However, it is also highly probable that, in addition to this nonreactive-collision mechanism, there are other processes involving reactions between the atoms and dimers taking place within the flow and these may lead to alignment as well.

B. Chemical exchange collisions

Evidence exists indicating that the chemical exchange process

$$\mathrm{Na}(1) + \mathrm{Na}(2)\,\mathrm{Na}(3) \rightarrow \mathrm{Na}(1)\,\mathrm{Na}(3) + \mathrm{Na}(2) \qquad (24)$$

occurs with ease. Crossed beam studies of Whitehead and Grice[35] on the alkali atom-dimer exchange reactions $\mathrm{M}' + \mathrm{M}_2 \rightarrow \mathrm{MM}' + \mathrm{M}$, where $\mathrm{M}' = \mathrm{Na}$ and K, and $M_2 = \mathrm{K}_2$, Rb_2, and Cs_2, show that the total reaction cross sections are on the order of 100 Å^2 or larger. Although these studies apply to mixed alkali atom-dimer exchange, it might be expected that comparable cross sections would be found for like alkali atom-dimer exchange reactions. Recently, Weber *et al.*[36] have reported the atom-dimer exchange cross section for $\mathrm{Cs}-\mathrm{Cs}_2$ to be 190 ± 40 Å^2, based on the relaxation rate of the nuclear spins in optically pumped Cs_2 dimers. Supporting evidence for these large cross sections has also been obtained by Gupta *et al.*[37] by the same method. Thus, Eq. (24) is a facile process, i.e., the cross section for chemical exchange is comparable to that for inelastic scattering. Therefore, chemical exchange collisions may help to account for the rapid vibrational and rotational cooling of the Na_2 dimers, as previously reported.[19]

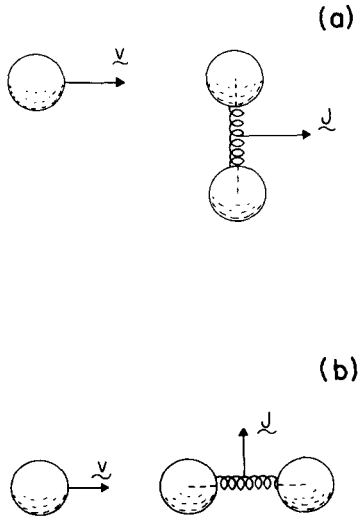

FIG. 9. Two extreme orientations for alkali atom-dimer exchange: (a) broadside approach; and (b) collinear approach.

The contribution which chemical exchange collisions make to the alignment comes about once again because of the angular dependence of the reaction cross section. As mentioned before, the dimer has azimuthal symmetry; hence the cross section will depend only on the angle which the relative velocity vector makes with the internuclear axis. One can visualize what could happen for two extreme orientations of the atom and dimer. Figure 9 illustrates these two cases, Fig. 9(a) depicting broadside attack by the atom and Fig. 9(b) indicating collinear attack. For the attacking atom to replace one of the atoms in the dimer, it is necessary that the force which it exerts be large enough to rupture the bond. Suppose the force which does this is a shearing force which acts as if to bend the molecule; then atom exchange will be more favorable in the case of Fig. 9(a) than in the case of Fig. 9(b). Since the force required is expected to be relatively large, only orientations within some small cone about the perpendicular to the internuclear axis might favor exchange in this crude classical treatment.

We now assume a dynamical situation similar to the one used for the hard-collision model, namely, that both the atoms and dimers move in the z direction, and the atoms move with a greater velocity than the dimers. Recalling that the angular momentum vector J always lies perpendicular to the internuclear axis, the preceding considerations indicate that those molecules with their J vectors lying along the beam axis will have a larger cross section to undergo exchange that those whose J vectors lie perpendicular to the beam axis (see Fig. 9). The result of this will be that those orientations of J along the beam axis will be depleted with respect to the other orientations, leading again to a distribution peaked at 90 deg to the beam axis. However, in this case, one would expect the distribution produced in the flow to be much broader about the perpendicular plane than that obtained from the hard collision model. The reason for this is that the range of orientations favoring exchange falls off rapidly as the collision deviates from broadside attack because of the requirement that the collision impulse have the necessary shear force required to rupture the bond. Such a distribution would more closely resemble the experimental distribution shown in Fig. 5. Of course, our classical treatment of chemical exchange is again over-simplified but, without detailed information on the dynamics of this pro-

cess, a more realistic treatment is not possible.

We are unable to estimate the relative contributions of the reactive and nonreactive processes to the alignment, and because the cross sections are comparable, we believe that both are operative. Although different, these processes are similar in two important respects; both depend on the angular part of the intermolecular potential and both require the presence of atomic and diatomic species. In a beam in which both these conditions are fulfilled, there is no reason to dismiss either process as unimportant. Despite the admittedly crude nature of both models, they do qualitatively account for the alignment of the molecules in the nozzle beam expansion and provide us with simple means of picturing a very complex process.

V. DISCUSSION

Ever since the experiments of Senftleben on thermal transport in the 1930's, it has been known that molecules undergo alignment in gaseous transport. There have been many indirect measurements of this effect, particularly by determining the change of transport coefficients under the application of external fields. Utilizing a nozzle beam expansion, which is characterized by a large pressure gradient, we have investigated the spatial distribution of angular momentum vectors of the molecules in such a beam using the degree of polarization of the molecular fluorescence as a probe. We have demonstrated that this new technique is perhaps the most sensitive and the most direct, as it measures the actual moments of the distribution and can detect very small concentrations of molecules. In particular, we have determined the relative contributions of the three leading Legendre polynomials to the distribution for a nozzle beam of sodium dimers. The distribution shows the expected behavior, namely, the angular momentum vectors of the molecules perferentially point away from the flow direction.

The alignment of the molecules can come about because the intermolecular potential is nonspherical for inelastic scattering and because the chemical exchange reaction depends on the relative orientation of the atom and dimer. We have developed a simple model based on the collisions between hard spheres and hard ellipsoids of revolution in order to picture the development of alignment of the molecules through inelastic collisions. This model suggests that alignment depends on the occurrence of "hard" collisions during the expansion in which the direction of the angular momentum vector of the molecule is randomized by the collision. We have also considered a simple classical model for chemical exchange which indicates that the process is highly anisotropic. We do not know the relative contributions of these two mechanisms to the alignment. To the extent that alignment occurs from inelastic processes, it should be enhanced by the presence of species of different mass and hence different velocity in the beam. This suggests that beam seeding techniques[17] might be used to promote alignment. To the extent to which chemical exchange processes cause alignment, it suggests that the expansion of mixtures which undergo chemical reaction will be useful in creating alignment.

The alignment of molecules in a supersonic expansion may be regarded as "translational optical pumping" in which the particles in the hydrodynamic flow act as a collisional state selector (filter) so that only molecules with a certain orientation and velocity "escape" into the beam. As in all optical pumping experiments, this effect may be employed to study either the spectroscopy or the collisional properties of the molecules. Thus we can imagine exploiting this state selection to aid the study of the molecular structure through electric beam resonance spectroscopy or to investigate the collisional properties of the state-selected molecules.[38] The latter possibility is particularly appealing in that nozzle beams may be used as a preselector for the electric field orientation of molecules[39,40] or they may be used directly in reactive scattering experiments to explore the dependence of the cross section on the orientation of the reactants (stereochemistry), thereby gaining information on the angular part of the intermolecular potential.[41] By the same token the interpretation of differential angular distribution data obtained from scattering experiments using nozzle beams as sources may need to be reassessed to account for the possibility that the nozzle beam molecules are aligned to some extent. However, it remains to be demonstrated whether nozzle expansion is or is not a general method for producing molecular alignment.

Alignment in gaseous transport is a ubiquitous phenomenon which may manifest itself in diverse circumstances. For example, the collisions between non-s-state atoms are characterized by an angle-dependent potential, and as first pointed out by Ramsey[42] and later observed by Toschek,[43] alignment may occur in atomic beams of such species. The same mechanism has been proposed by Gold[44] to explain the polarization of the star light propagating through the interstellar medium. It is postulated that collisions between nonspherical grains moving at supersonic velocities and interstellar gas atoms cause alignment of the grains. Another context where alignment may occur and which appears not to have been previously mentioned in the literature is the extraction of atomic and molecular ions from high-pressure sources under the influence of an electric field.[45] We do not know how to assess the consequences such effects may have had on previous ion mobility studies and angular distribution studies carried out on ions extracted from such sources. However, it is possible that this technique offers the opportunity for preparing aligned species under controlled conditions.

Chemical reactions under beam conditions are already known to produce products which are preferentially aligned in a plane perpendicular to the initial relative velocity vector. This alignment has been detected for chemiluminescent reactions by observing the degree of polarization of the emission from the products.[26] Most recently, Maltz, Weinstein, and Herschbach[46] and Hsu and Herschbach[47] have applied electric deflection techniques to determine the degree of alignment of polar alkali halide products formed in the reactions of various alkali metals with halogen-containing compounds. The

difference between the deflection profiles (measure of anisotropy) obtained with an inhomogeneous electric field oriented parallel and perpendicular to the plane of the reactant beams is characterized by an expansion in even-ordered Legendre polynomials $1+a_2P_2(\cos\chi)+\ldots$ where χ is the angle between the product rotational angular momentum and the initial relative velocity vector. The profile differences are found to depend primarily on the coefficient a_2 but in some cases the a_4 coefficient can be determined as well. In an analogous manner degree of polarization studies of resonance fluorescence from the product molecules, as described here, can yield comparable information.

The same mechanism which leads to alignment in gaseous transport may also produce orientation ($+M_J$ and $-M_J$ sublevels unequally populated) provided that the molecule has a different scattering or reactive cross section, depending on orientation. While this is not possible for any $^1\Sigma$ homonuclear molecule such as Na_2, these effects might be expected to appear in a gas transport process involving heteronuclear diatomic molecules or polyatomic molecules whose shapes may be characterized by a "bow" and a "stern." The extent of orientation may be found from measuring the degree of circular polarization of the fluorescence, just as the extent of alignment is obtained by measuring the degree of linear polarization of the fluorescence.

ACKNOWLEDGMENTS

We thank S. H. Bauer, B. Berne, R. Bersohn, J. B. Fenn, and P. Pechukas for stimulating and enlightening discussions on the model for collisional alignment. Support by the National Science Foundation under grant NSF-GP-31336 is gratefully acknowledged.

*Present address: Department of Engineering and Applied Science, Yale University, New Haven, CT 06520.
†Graduate student, Department of Physics, Columbia University, New York, NY 10027.

[1]J. C. Maxwell, Proc. R. Soc. A **22**, 46 (1873); Pogg. Ann. Phys. **151**, 151 (1874).
[2]H. Senftleben, Phys. Z. **31**, 822, 961 (1930).
[3]J. J. M. Beenakker, G. Scoles, H. F. P. Knaap, and R. M. Jonkman, Phys. Lett. **2**, 5 (1962).
[4]For a review and further references see J. J. M. Beenakker and F. R. McCourt, Ann. Rev. Phys. Chem. **21**, 47 (1970).
[5]L. Waldmann, Z. Naturforsch. A **12**, 660 (1957); **13**, 609 (1958); Acta Phys. Aust. Suppl. **10**, 223 (1973).
[6]R. F. Snider, J. Chem. Phys. **32**, 1051 (1960); R. F. Snider and B. C. Sanctuary, *ibid.* **55**, 1555 (1971).
[7]L. Waldmann, Nuovo Cimento **14**, 898 (1959); Z. Naturforsch. A **15**, 19 (1960).
[8]Y. Kagan and A. M. Afanasev, Zh. Eksp. Teor. Fiz. **41**, 1536 (1961) [Sov. Phys.—JETP **14**, 1096 (1962)].
[9]R. G. Gordon, J. Chem. Phys. **44**, 3083 (1966); **45**, 1649 (1966).
[10]V. G. Cooper, A. D. May, E. H. Hara, and H. F. P. Knaap, Can. J. Phys. **46**, 2019 (1968); S. Hess, Phys. Lett. A **29**, 108 (1969); Z. Naturforsch. A **25**, 350 (1970); R. A. J. Keijser, M. Jansen, V. G. Cooper, and H. F. P. Knaap, Physica **51**, 593 (1971).
[11]R. G. Gordon, J. Chem. Phys. **44**, 228 (1966); J. L. Kinsey, J. W. Riehl, and J. S. Waugh, *ibid.* **49**, 5269 (1968); J. W. Riehl, J. L. Kinsey, J. S. Waugh, and J. H. Rugheimer, *ibid.* **49**, 5276 (1968); P. A. Speight and R. L. Armstrong, Can. J. Phys. **47**, 1475 (1969).
[12]G. Birnbaum, *Intermolecular Forces*, edited by J. O. Hirschfelder (Wiley, New York, 1967), p. 539.
[13]S. Hess, Phys. Lett. A **30**, 239 (1969); Acta Phys. Aust. Suppl. **10**, 247 (1973).
[14]F. Baas, Phys. Lett. A **36**, 107 (1971).
[15]C. J. Gorter, Naturwiss. **26**, 140 (1938).
[16]J. I. Steinfeld, Department of Chemistry, Massachusetts Institute of Technology, Cambridge, MA 02139 and J. Korving, Kamerlingh Onnes Laboratorium, Leiden, Nederland (private communications).
[17]For reviews on nozzle beams see J. B. Anderson, R. P. Andres, and J. B. Fenn, Adv. Chem. Phys. **10**, 275 (1966); and T. A. Milne and F. T. Greene, *Advances in High Temperature Chemistry*, edited by LeRoy Eyring (Academic, New York, 1969), Vol. II, p. 107.
[18]A. H. Shapiro, *The Dynamics and Thermodynamics of Compressible Fluid Flow* (Ronald, New York, 1953), Vol. I, Chap. 4.
[19]M. P. Sinha, A. Schultz, and R. N. Zare, J. Chem. Phys. **58**, 549 (1973). For further information, see M. P. Sinha, Ph.D. thesis, Columbia University, New York, NY 10027.
[20]P. Pringsheim, *Fluorescence and Phosphorescence* (Interscience, New York, 1965).
[21]P. P. Feofilov, *The Physical Basis of Polarized Emission* (Consultants Bureau, New York, 1961).
[22]R. N. Zare, J. Chem. Phys. **45**, 4510 (1966).
[23]W. Demtröder, M. McClintock, and R. N. Zare, J. Chem. Phys. **51**, 5495 (1969).
[24]R. E. Drullinger and R. N. Zare, J. Chem. Phys. **51**, 5532 (1969); **59**, 4225 (1973).
[25]The degree of polarization is independent of the vibrational member of the fluorescence series observed. See Ref. 21.
[26]This is an improved version of the rotating polarizer described in C. D. Jonah, R. N. Zare, and Ch. Ottinger, J. Chem. Phys. **56**, 263 (1972).
[27]An. N. Nesmeyanov, *Vapor Pressure of the Elements* (Academic, New York, 1963).
[28]H. D. Young, *Statistical Treatment of Experimental Data* (McGraw-Hill, New York, 1962).
[29]R. J. Gordon, Y. T. Lee, and D. R. Herschbach, J. Chem. Phys. **54**, 2393 (1971).
[30]N. Abuaf, J. B. Anderson, R. P. Andres, J. B. Fenn, and D. R. Miller, Adv. Appl. Mech., Suppl. **4**, 2, 1317 (1967).
[31]J. Jennings, *The Reynold's Number* (Emmott, London, 1946).
[32]Similar classical collisions between nonspherical molecules have been used by Y. Ishida [Phys. Rev. **10**, 305 (1917)] and C. F. Curtiss and co-workers to derive a Boltzmann Equation for polyatomic molecules with internal angular momentum as an additional degree of freedom. [J. Chem. Phys. **24**, 225 (1956); **26**, 1619 (1957)].
[33]At first glance there appears to be a contradiction in that the molecules become rotationally cooler by collisions in the expansion process whereas hard collisions have the tendency to rotationally heat the molecules. However, it should be borne in mind that there are many more soft collisions than hard collisions, and the soft collisions play the role of maintaining the rotational degree of freedom of the molecule at the "ambient temperature" of the beam without effectively changing the orientation of J.
[34]The 4° divergence of the beam causes the apparent distribution to be slightly flatter than the actual distribution, but calculations show that this does not account for the difference between Figs. 5 and 8.
[35]J. C. Whitehead and R. Grice, Faraday Disc. Chem. Soc. **55**, 320 (1973).
[36]H. G. Weber, H.-J. Glas, R. Huber, M. Kompitsas, G. Schmidt and G. zu Putlitz, Z. Physik (to be published).
[37]R. Gupta, W. Happer, G. Moe, and W. Park, Phys. Rev. Lett. **32**, 574 (1974).
[38]S. Stolte, thesis, Nijmegen, 1972; S. Stolte, J. Reuss, and

H. L. Schwartz, Physica **66**, 211 (1973); W. Franssen and J. Reuss, *ibid.* **63**, 313 (1973).
[39]R. J. Beuhler, Jr., R. B. Bernstein, and K. H. Kramer, J. Am. Chem. Soc. **88**, 5331 (1966); R. J. Beuhler, Jr., and R. B. Bernstein, Chem. Phys. Lett. **2**, 166 (1968); R. J. Beuhler, Jr., and R. B. Bernstein, J. Chem. Phys. **51**, 5305 (1969).
[40]P. R. Brooks and E. M. Jones, J. Chem. Phys. **45**, 3449 (1966); P. R. Brooks, *ibid.* **50**, 5031 (1969); P. R. Brooks, E. M. Jones, and K. Smith, *ibid.* **51**, 3073 (1969); E. M. Jones and P. R. Brooks, *ibid.* **53**, 55 (1970).
[41]H. G. Bennewitz, K. H. Kramer, W. Paul, and J. P. Toennies, Z. Physik **177**, 84 (1964); H. G. Bennewitz, R. Haerten, and G. Müller, *ibid.* **226**, 139 (1969); H. G. Bennewitz, R. Gengenbach, R. Haerten, and B. Müller, *ibid.* **227**, 399 (1969); K. Berkling, R. Helbing, K. Kramer, H. Pauly, Ch. Schlier, and P. Toschek, *ibid.* **166**, 406 (1962).
[42]N. F. Ramsey, Phys. Rev. **98**, 1853 (1955).
[43]P. Toschek, Z. Physik **187**, 56 (1965).
[44]T. Gold, Nature **169**, 322 (1952). See also J. Mayo Greenberg, "Interstellar Grains," Chap. 6 in *Nebulae and Interstellar Matter*, edited by B. M. Middlehurst and L. H. Allen (Vol. VIII of Stars and Stellar Systems, Univ. of Chicago Press, 1968); E. M. Purcell, Physica **41**, 100 (1969).
[45]E. W. McDaniel, *Collision Phenomena in Ionized Gases* (Wiley, New York, 1964), Chap. 9.
[46]C. Maltz, N. D. Weinstein, and D. R. Herschbach, Mol. Phys. **24**, 133 (1972).
[47]D. S. Y. Hsu and D. R. Herschbach, Faraday Disc. Chem. Soc. **55**, 116 (1973).